The Normalization of Surface Anisotropy Effects Present in SEVIRI Reflectances by Using the MODIS BRDF Method

Simon Richard Proud, Qingling Zhang, Crystal Schaaf, *Member, IEEE*, Rasmus Fensholt, Mads Olander Rasmussen, Chris Shisanya, Wycliffe Mutero, Cheikh Mbow, Assaf Anyamba, Ed Pak, and Inge Sandholt

***Abstract*—A modified version of the MODerate resolution Imaging Spectroradiometer (MODIS) bidirectional reflectance distribution function (BRDF) algorithm is presented for use in the angular normalization of surface reflectance data gathered by the Spinning Enhanced Visible and InfraRed Imager (SEVIRI) aboard the geostationary Meteosat Second Generation (MSG) satellites. We present early and provisional daily nadir BRDF-adjusted reflectance (NBAR) data in the visible and near-infrared MSG channels. These utilize the high temporal resolution of MSG to produce BRDF retrievals with a greatly reduced acquisition period than the comparable MODIS products while, at the same time, removing many of the angular perturbations present within the original MSG data. The NBAR data are validated against reflectance data from the MODIS instrument and *in situ* data gathered at a field location in Africa throughout 2008. It is found that the MSG retrievals are stable and are of high-quality across much of the SEVIRI disk while maintaining a higher temporal resolution than the MODIS BRDF products. However, a number of circumstances are discovered whereby the BRDF model is unable to function correctly with the SEVIRI observations—primarily because of an insufficient spread of angular data due to the fixed sensor location or localized cloud contamination.**

***Index Terms*—Angular effects, anisotropy, bidirectional reflectance distribution function (BRDF), land surface reflectance, MODerate resolution Imaging Spectroradiometer (MODIS), Meteosat Second Generation (MSG) Spinning Enhanced Visible and InfraRed Imager (SEVIRI).**

Manuscript received September 10, 2013; revised October 26, 2013; accepted November 12, 2013.

S. R. Proud, R. Fensholt, and M. O. Rasmussen are with the Department of Geosciences, University of Copenhagen, 1350 Copenhagen, Denmark (e-mail: srp@geo.ku.dk).

Q. Zhang is with the School of Forestry and Environmental Studies, Yale University, New Haven, CT 06511 USA.

C. Schaaf is with the Environmental, Earth and Ocean Sciences Department, University of Massachusetts Boston, Boston, MA 02125 USA.

C. Shisanya is with the Department of Geography, Kenyatta University, GPO 00100 Nairobi, Kenya.

W. Mutero is with the Kenya Wildlife Service, GPO 00100 Nairobi, Kenya.

C. Mbow is with the Université Cheikh Anta Diop, Institut des Sciences de l'Environnement, BP 5005 Dakar, Senegal.

A. Anyamba is with the Hydrological and Biospheric Sciences, NASA Goddard Space Flight Center, Greenbelt, MD 20771 USA.

E. Pak is with Science Systems Applications, NASA Goddard Space Flight Center, Greenbelt, MD 20771 USA.

I. Sandholt is with the Division of Microwaves and Remote Sensing, Danish Technical University Space, Copenhagen, Denmark.

Color versions of one or more of the figures in this paper are available online at http://ieeexplore.ieee.org.

Digital Object Identifier 10.1109/TGRS.2013.2294602

I. Introduction

IT IS WELL documented that, when measured by a space-based instrument, the reflectance of the Earth's land surface displays a dependence, known as anisotropy, upon the illumination and viewing geometry between the sun, target, and sensor [1], [2]. The effectiveness of comparing reflectances over differing time periods or locations to detect change is reduced unless such directional effects can be minimized. Typically, this is achieved through the use of a bidirectional reflectance distribution function (BRDF) that describes this angular dependence as a function of the viewing and illumination conditions [3], [4] and can therefore be used to produce reflectances that are normalized to a common set of solar and viewing angles. This enables a much more accurate intercomparison between different locations and times of year. It can also be described as a technique to remove the influence of scene geometry from the remotely sensed data series. Given a selection of remotely sensed surface reflectances and their associated angular parameters, it is possible to estimate the BRDF for a particular land surface using a model [5], [6], and there are various such models available, including the Roujean model [7], the RossThick LiSparseR (RTLSR) model [8], [9], Walthall's model [10], Minnaert's model [11] or the Rahman–Pinty–Verstraete model [12]–[14]. These models are commonly applied to remotely sensed data gathered from polar-orbiting sensors such as the MODerate resolution Imaging Spectroradiometer (MODIS) [15], Multiangle Imaging SpectroRadiometer (MISR) [14], [16], [17], Polarization and Directionality of the Earth's Reflectances [18]–[20], and VEGETATION [21] due to the wide range of angular conditions that these sensors encounter. These gather data over a time period spanning several days, typically 8–16, for use in generating one BRDF, resulting in a high-quality product—but one in which rapid land surface changes due to precipitation, fires, etc., may not be visible. In areas such as the Sahel that undergo rapid greening of vegetation during the rainy season, this 16-day retrieval time may be too long to monitor the greening as it occurs. The BRDF models are sensitive to the quantity of input observations made under differing geometrical conditions, with more observations over a wide range of conditions typically resulting in a higher quality BRDF product. As polar-orbiting sensors—with the notable exception of MISR—only gain one or two looks at a particular land surface per day, a long acquisition period is usually required to build up a sufficient number of observations for the BRDF model to be successful.

However, through the use of geostationary sensors, such as the Meteosat Visible and Infrared Imager on board Meteosat [22], [23] or the Spinning Enhanced Visible and InfraRed Imager (SEVIRI) aboard Meteosat Second Generation (MSG), that produce surface reflectance information over a wide area, known as the full disk, at a much higher temporal resolution, it is possible to generate BRDF data, and hence normalized reflectances, on a more timely basis [24], [25]. The repeated views of a scene during one day result in a large spread of illumination conditions, something that is very useful when generating a reliable BRDF model [26]. This is, however, counterbalanced by the fixed viewing geometry that is inherent to any geostationary platform, something that can result in a reduction in anisotropic variation within an observed reflectance time series. The European Land Surface Applications Facility (LandSAF) computes BRDF-adjusted albedos based upon the SEVIRI data on a daily timescale [24], [25], [27]. As well as these daily products, the LandSAF also produces a ten-day albedo product. These products have been well validated and found to give good-quality albedo data for the African continent. However, at the time of writing, the BRDF weighting parameters are not available as an online product, which means that research involving these parameters is not possible with the LandSAF data. A secondary issue is that LandSAF only disseminates data for particular regions of interest, Africa, Europe, and South America, meaning that no BRDF is available for some areas of the SEVIRI full disk, such as the Middle East. Additionally, the acquisition period, input data quality, and internal accuracy thresholds are all fixed. This results in an accurate and easy-to-use end product, but in cases where more flexibility is required, it is advantageous to use an alternative BRDF code that allows the user to tailor the algorithm to their particular purposes.

The MODIS Land Science Team has released a version of the MODIS BRDF algorithm specifically for the needs of the direct broadcast (DB) community. Members of this community are typically attempting to monitor regional conditions on a weekly or daily basis for rangeland, crop, or timber management. This version of the algorithm allows the specification of variable retrieval periods and tailoring of the various quality thresholds to a specific locality. Therefore, within this study, a modified version of the MODIS DB BRDF algorithm [4] is applied to data gathered using SEVIRI in an attempt to produce daily BRDF-adjusted land surface reflectances for the full SEVIRI disk. These are modeled in the style of the MODIS nadir BRDF-adjusted reflectance (NBAR) product so that the sensor appears nadir to the target pixel while the sun is positioned at the zenith angle equivalent to local solar noon. In addition to NBAR values, the SEVIRI BRDF algorithm also outputs BRDF kernel weighting parameters that can be used to model reflectance values under any geometric conditions. These parameters can also be of use in their own right, for example, in examining vegetation [28]. The BRDF-adjusted SEVIRI reflectances are compared to the equivalent data from the well-established MODIS-derived BRDF product for the year 2008. A comparison is also made to *in situ* data gathered at a field location in Africa. This provides a direct validation method in addition to intercomparison with other satellite remote sensing instruments. Details of the MSG/SEVIRI system and of the MODIS BRDF method are given in Sections II and III, respectively, while the method and justification for comparing MSG-BRDF reflectances to the MODIS and *in situ* data are explained in Section IV.

II. Data Used Within This Study

A. MSG SEVIRI Reflectance Data

The SEVIRI instrument is aboard the MSG-1, -2, and -3 spacecraft that are located in geostationary orbit, with the primary spacecraft, MSG-3, nominally positioned at 0° longitude. The backup MSG-2 is positioned at 9.5°E but is unused within this study. MSG-1 was the first MSG to be launched and is currently a backup satellite that can be used in the event of a failure aboard MSG-2 or -3. From the position over the equator, the SEVIRI sensor views much of Europe, all of Africa, the Eastern parts of the Americas, and the majority of the Middle East. Due to the fixed satellite position and unlike polar-orbiting instruments, the viewing angles do not change with time, meaning that the view zenith angle (VZA) and view azimuth angle (VAA) of each pixel can be precomputed and stored. SEVIRI is a multispectral sensor that gathers radiance information in 12 wavelength bands from the visible to the infrared (IR) with a 15-min repeat cycle at a 3-km spatial resolution near the subsatellite point. Within this study, the focus is upon the three visible and near-IR (VNIR) channels—known as channels 1, 2, and 3—that are centered upon 635, 810, and 1640 nm, respectively [29]. These bands can be used for cloud detection, the examination of aerosol optical depth (AOD), soil moisture content, or the derivation of vegetation parameters such as the Normalized Difference Vegetation Index (NDVI) and Shortwave Infrared Water Stress Index [30]–[34].

The 15-min temporal resolution provides a large quantity of data per day that will, depending upon latitude, typically result in up to 50 sunlit observations for each pixel. However, some of these may be of poor quality due to prolonged cloud or aerosol contamination, particularly in regions such as Central Africa. Between each 15-min period, the sun will move by approximately 3.75°, providing a large range of solar zenith and azimuth angles (SZA and SAA) for input into the BRDF model. Due to the reciprocal nature of the RTLSR BRDF model that allows solar and viewing geometry to be interchanged, these varying solar angles can be useful in overcoming the limit of fixed viewing angles. SEVIRI data are received using the EUMETCAST system [35] and stored locally. Data are received as raw digital counts and are preprocessed first into radiance and then into reflectance using calibration information embedded in the data stream. Then, both the European Organisation for the Exploitation of Meteorological Satellites cloud mask [36] and the Satellite Applications Facility in Support on Support to Nowcasting & Very Short Range Forecasting cloud mask [37] are applied to the raw data, and atmospheric correction is performed using a modified version of the SMAC code [38]–[40]. As the atmospheric correction requires knowledge of the AOD, water vapor, and ozone content, this information is fed into the SMAC from the relevant MOD08/MYD08

MODIS atmosphere products on a daily basis. We interpolate between values retrieved from the MODIS instruments aboard Terra and Aqua to produce a single value for each pixel and each atmospheric parameter. Using a daily atmosphere product degrades the accuracy of surface reflectance information, as it is impossible to correct for rapid diurnal changes in atmospheric conditions, but no equivalent products are available on the MSG 15-min temporal resolution. Nevertheless, preprocessing the data in this way eliminates much of the noise due to cloudiness or atmospheric effects and provides a much clearer indication of the underlying surface anisotropy.

B. MODIS Reflectance Product

The MODIS MCD43A4 16-day NBAR product [41] is used for comparison with MSG-BRDF data. This utilizes the same angular correction method as used within this study, but applied to data gathered by the MODIS instrument aboard Aqua and Terra on a series of $10 \times 10^{\circ}$ tiles at a 500-m spatial resolution [4]. A 16-day retrieval timescale is used within the MCD43A4 product to ensure that adequate numbers of cloud-free observations under sufficiently different geometrical conditions are acquired for each pixel. A retrieval is attempted every 8 days, and therefore, two 16-day retrievals are provided per 24-day period, with one covering days 1–16 and the other covering days 8–24. This overlap allows for smoother changes in the modeled land surface reflectance over time and also increases the timeliness of the NBAR response to sudden changes in the observed land surface. The MODIS reflectance product is atmospherically corrected using the 6S method [42], [43]. The MODIS cloud masks are used to remove cloud contamination, and the surface reflectance data are automatically examined for cloud contamination, with reflectance values that appear as outliers during the BRDF retrieval being removed from processing and thus not affecting the final BRDF computation. The MODIS BRDF/albedo product has been validated over a number of regions [44]–[52] and consequently is a reliable source from which to judge the accuracy and stability of the MSG-derived BRDF values, although due to the slightly different spectral response functions of the instruments, it is expected that some differences in reflectance will be present.

C. Dahra Field Site

The Dahra (15.44°N, 15.45°W) field site hosts various sensors simulating SEVIRI channels 1 and 2 that can be used for comparison with those retrieved by the satellite (e.g., [33]). This site is in the Sahel region and has two seasons—the dry season from November to June and a wet season that runs between July and October [53]. These two seasons mean that two very different distributions of NDVI values are observed: Those in the dry season will be low (around 0.15–0.25), and those from the wet season will be significantly higher (above 0.6). There is a period of two to three weeks in which the NDVI transitions from low to high and then a much longer transition at the end of the wet season where the NDVI returns to low values. After the end of the wet season in late October, it will normally take until early January before the NDVI returns to around 0.2.

To allow comparison with the satellite observations, the site was mapped to its corresponding MSG pixel. The satellite pixel covers a much wider area of ground (approximately 16 km^2) than the field sensors, and a result of this scaling will be small differences in the measured values between ground and space. The field site was found to be close to the southern edge of the SEVIRI pixel, and the sensors point at an area that, depending upon the time of year, is mainly grassland or bare soil. Tree cover for the MSG pixel is less than 5% with all of the trees being outside of the *in situ* sensor field of view [54]. This landscape is fairly typical of the MSG pixel, and as the tree cover in the area is low, it is expected that having no trees close to the *in situ* sensors will not significantly affect the results of a point to pixel comparison [55]. The field site collected data from January to late October 2008, with some days of missing data in May and July due to maintenance at the field site. Here, we compare NDVI values rather than reflectances as the sensors were calibrated to produce accurate NDVI values. This means that, when comparing reflectances, the sensors sometimes give abnormally high or low values. By using NDVI, we gain the most accurate *in situ* data, and because NDVI is simply a combination of two channels of reflectance data, we can still analyze the effectiveness of the BRDF method.

The existence of subpixel clouds that are too small to be picked up by the SEVIRI cloud masks will also affect the comparison between ground and space data sources. Despite their small size, subpixel clouds can dramatically affect the measured reflectance, particularly that measured by the SEVIRI instrument due to its relatively low spatial resolution. Ground-based sensors are subject to a much smaller amount of interference from the atmosphere than their space-based equivalents, but an attempt is made to minimize the effects of the atmosphere as the SEVIRI data used within this study are cloud cleared and atmospherically corrected.

III. BRDF Correction Method

In order to produce NBAR data from MSG SEVIRI reflectances, a modified version of the MODIS DB BRDF algorithm is used [4], [9]. This method expands the BRDF into a linear sum of three terms, or kernels, that each partially describes the dependence of land surface reflectances upon the viewing and illumination geometry as a function of different scattering modes. The MODIS BRDF model utilizes three kernels that represent the modes: isotropic scattering, volumetric scattering, and geometric scattering. This means that a reflectance value can be modeled as a function of these three terms

$$R(\theta, \vartheta, \phi, \Lambda) = f_{iso}(\Lambda) + f_{vol}(\Lambda) K_{vol}(\theta, \vartheta, \phi) + f_{geo}(\Lambda) K_{geo}(\theta, \vartheta, \phi). \quad (1)$$

In the above equation, $\mathrm{R}(\theta, \vartheta, \phi, \Lambda)$ represents a modeled reflectance for a wavelength Λ made at solar and viewing zenith angles θ and ϑ and relative azimuth angle given by ϕ. f is the model weighting parameter associated with each kernel and for each wave band while the actual kernel value is denoted by K. These kernel values are independent of the input reflectances and vary as a function of only the scene geometry, enabling them to be precomputed and stored in a lookup table if desired.

The MODIS BRDF algorithm employs the RossThick kernel first proposed by Roujean *et al.* [7], [56] for the volumetric kernel that assumes a relatively dense canopy and does not account for multiple scattering. This single scattering approximation is valid for cases in which the absorptivity of the target surface is high (such as for a canopy within the visible region of the spectrum). However, for the near-IR spectral region, this approximation becomes less valid, but it has been shown that additional scattering events exhibit a greatly reduced angular dependence and tend to produce an additional isotropic contribution to the measured reflectance [57]. It is therefore still a valid assumption to only include the single scattering case, although including an additional kernel such as LiSparse may provide a better modeling of this contribution. To account for geometric scattering, the Li-SparseR kernel is used [58], and it proposes a selection of objects positioned sparsely across the observed surface, which is assumed to be a Lambertian reflector. The original formulation of this kernel was not reciprocal in solar and viewing zenith angles, as the component reflectances were not assumed to be constant for varying solar zenith angle, something that is not expected to be true for data gathered at the spatial resolution and positioning of the MODIS or SEVIRI sensors [59]. By adding a simple term to account for the variation in reflectance due to shifting solar zenith angle, it is possible to transform this kernel into the reciprocal Li-SparseR kernel. Although the kernel values are independent of the observed reflectances, the model parameters are not. Meaning that information on both the surface reflectance and the scene geometry is required to calculate these parameters. Within the MODIS BRDF algorithm, this is achieved by minimizing a least squares error function

$$e^2(\Lambda) = \frac{1}{d}\sum_{i=0}^{n}\frac{\left[\rho(\theta_i,\vartheta_i,\phi_i,\Lambda) - R(\theta_i,\vartheta_i,\phi_i,\Lambda)\right]^2}{\omega_i(\Lambda)} \tag{2}$$

where ρ is an input reflectance at a given set of solar, viewing, and relative azimuth angles (θ_i, ϑ_i, and ϕ_i, respectively), n is the total number of observations recorded, and d denotes the degrees of freedom. For this BRDF model, the degrees of freedom are equal to $n-3$, as three kernels are used. Inverting this function results in an analytical solution for the model weighting parameters. The term $\omega_i(\Lambda)$ is a weight that is assigned to each input observation. Within the original MODIS BRDF implementation, this weight was dependent upon various input parameters, such as the aerosol loading, cloud type present over a pixel, and whether the land surface is shadowed. Such detailed information is not available within the MSG-BRDF method, however, so a simple weighting, similar to that described by Geiger *et al.* [27], was used instead

$$\omega_i(\Lambda) = \frac{2}{\left(\frac{1}{cos(\theta_i)} + \frac{1}{cos(\vartheta_i)}\right)}. \tag{3}$$

This scheme will give more weight to observations gathered at low VZA or SZA and, in testing, was found to produce smaller uncertainties than the case if no weighting was used. In addition to the weighting of observations, a method is also employed to remove noisy reflectances from the set of input data. A quality flag is used to denote good or bad input observations. Should any observation be flagged as cloudy within the MSG cloud masks or fail one of the tests described in (4)–(7), then it will fail the quality testing, be flagged as bad data, and be ignored by the BRDF calculation. If the following tests are passed, then the data are described as suitable for use:

$$0 < \rho(\theta_i,\vartheta_i,\phi_i,\Lambda) < 1 \tag{4}$$

$$0.85 < \frac{\rho(\theta_i,\vartheta_i,\phi_i,\Lambda)}{\rho(\theta_{i-1},\vartheta_{i-1},\phi_{i-1},\Lambda)} < 1.15 \tag{5}$$

$$0.85 < \frac{\rho(\theta_i,\vartheta_i,\phi_i,\Lambda)}{\rho(\theta_{i+1},\vartheta_{i+1},\phi_{i+1},\Lambda)} < 1.15 \tag{6}$$

$$\theta_i < 70^\circ \; and \; \vartheta_i < 70^\circ. \tag{7}$$

Equation (4) checks that the input reflectance is within a sensible range while (5) and (6) examine two concurrent observations to determine if either is markedly different from the other. If there is a difference of greater than 15%, then it is assumed that the observation is cloud contaminated, and it is then removed from the processing chain. Finally, (7) checks that the SZA and VZA fall below 70° as, beyond this value, the atmospheric correction scheme is of reduced accuracy and the BRDF model may no longer be suitable.

Once the input observations have been tested for suitability, they are processed through the BRDF algorithm in accordance with (1). When deriving the model parameters from the input observations, the model is said to be operating in "backward mode" in which the model is inverted. Once the parameters have been determined, it is then possible to operate the model in "forward mode" and compute the modeled reflectance for any combination of solar and viewing conditions. In order to determine the accuracy and success of the model inversion, several quality flags are derived in addition to the kernel parameters. If any of the quality values are found to be outside of a predetermined range, then the inversion is said to have failed, and no parameters are recorded. The first of these is the root-mean-square error (RMSE) value associated with each pixel and calculated using (2).

For a perfect inversion, the RMSE would be zero, although due to factors such as sensor performance, atmospheric effects, and the slight inability of the BRDF model to fit the observed reflectances, the RMSE will almost always be nonzero. The RMSE is compared to a predefined reference value of 0.1 [60], with only inversions resulting in RMSEs that are lower than this value being deemed of acceptable quality. Two other quality flags, called the weights of determination (WoDs) [26], are also computed. The WoDs are an important determinant of BRDF model fit quality and are essentially a ratio of the noise introduced by the BRDF model compared to the noise present within the input reflectances. If the WoD value is greater than 1, it indicates that the BRDF model is amplifying noise, while values of less than 1 indicate that it is suppressing noise.

One of these, known as the NWoD, is similar to the typical output product, NBAR, but with the sun located at a 45° zenith angle rather than at local solar noon. The sensor is still modeled to be nadir to the observed surface. The second WoD is based upon the white sky albedo (WSAWoD). As with the

RMSE quality test, the WoDs for a pixel are compared to a precomputed set of acceptable values, and a series of threshold values is introduced to determine if the inverted BRDF model is of good quality. For the NWoD case, this threshold value is 1.25, and for the WSAWoD, the threshold is 2.5. If either of these, or the RMSE threshold, is exceeded, then the inversion is regarded as poor, and the BRDF is discarded.

In the case of the operational MODIS algorithm, a backup inversion method is used. This method, also known as a magnitude inversion, utilizes a database of seasonal BRDF weighting parameters for each pixel within a scene. The BRDF model for these parameters is then scaled according to the magnitude of any available MODIS reflectances. This magnitude inversion enables the extraction of NBARs even if a full inversion is not possible—but it does rely on historical BRDF weighting values and is thus prone to errors if the land surface changes since the database was last updated. Within this study, the MSG implementation of the magnitude inversion is inactive and so will not be included in the results.

Due to the differing spectral response of the land surface at different wavelengths, this inversion process is performed independently for each band, resulting in separate NBAR and parameter values for MSG channels 1, 2, and 3. The actual inversion method is identical between bands, with the only difference being the set of input reflectances that are used.

Once the MSG-BRDF algorithm has completed both the backward inversion and the forward reflectance derivation, it saves the NBARs for channels 1, 2, and 3 as well as the associated model parameters and quality information. This allows for comparison to other data sources such as MODIS that also generate NBARs, as well as for later computation of the reflectance and albedo at other scene geometries.

IV. Intercomparison Method

Within this study, the VNIR reflectance values from MODIS (channels 1, 2, and 6) and SEVIRI (channels 1, 2, and 3) instruments are used. Each sensor has a similar spectral response in these bands, although some differences do exist between them, which will cause small disagreements between the MODIS and SEVIRI reflectances that are not a result of the BRDF adjustment process. This is not likely to present a problem in determining the quality of the MSG-BRDF algorithm; however, as the BRDF method is identical between wavelength bands, the only difference is the set of input reflectances that is used to generate the BRDF model. Therefore, the stability of the algorithm can be assessed, even if the final reflectances are not directly comparable.

To compare the MODIS and SEVIRI reflectances, the two data sets must be scaled to the same spatial and temporal resolution. Additionally, as the MSG magnitude inversion technique is unused here, it was decided that only full inversions from both the MSG and MODIS algorithms should be compared. The MCD43A2 BRDF quality product was therefore used to determine which pixels produced a full inversion within each 16-day period, and all other pixels within a tile (those with no reflectance and those with a magnitude inversion) were masked to prevent their usage within the analysis. These masked tiles at a 500-m resolution were then mosaiced to form a single image for the whole of the SEVIRI disk before being resampled by the Geospatial Data Abstraction Library tools to match the spatial resolution and geostationary projection of the SEVIRI reflectance data. The final preprocessing step was to mask out water areas. Both the MODIS and SEVIRI data are water masked prior to the BRDF inversion, but due to differences in the water mask used by the two data sets, an additional water mask was applied. This masked out all pixels within 4 km of the coastline (1 MSG pixel and 8 MODIS pixels) and applied a 3×3 pixel mask (after resampling to MSG resolution) to all rivers and lakes—thus removing them from the data set. As the MSG-BRDF model uses a daily acquisition period, each 16-day MODIS scene is covered by 16 MSG-BRDF images, meaning that MSG scenes must be combined to form one 16-day scene. The minimum and maximum values found within the MSG-BRDF retrievals were removed, and the mean of the remaining retrievals was calculated for comparison with the MODIS data. By performing the data reduction in this way, it is expected that the errors present due to residual cloud contamination will be reduced. Also, at times when rapid greening occurs, this approach will capture a snapshot of the reflectance that more closely matches that produced by MODIS. Using an average of all four retrievals tends to bias the results in favor of pre- or postgreening conditions. Once this step was performed, the 16-day NBAR series were compared to examine the quality of fit between satellites, initially by computing the relative difference between methods.

A comparison was also carried out between the *in situ* data gathered at the field site, the MSG-BRDF data, and the MODIS values. The BRDF reflectances were examined, and data were extracted for the pixel corresponding to the field site, but in this case, the MODIS data were not resampled, so the original 500-m reflectances were used. As the field sites gather data on a 15-min repeat cycle, a processing scheme was applied in order to derive daily reflectance data. This processing scheme identified cloud contamination (using the MSG cloud mask as well as local data regarding solar illumination) and also removed any bad data due to other effects. Bad data were identified by using a four-day average and standard deviation, and any data that fell outside of $\mu \pm \sigma$ were deemed as bad quality and removed from the comparison. All remaining data were then averaged to produce the four-day field NDVI. Examination of this time series showed that it resulted in a smooth NDVI with only a few fluctuations due to noise or other effects and is therefore very suitable for use in a comparison study with the MSG data. This bad data removal process only resulted in three days of field data, all in July, being masked. The remaining days were deemed of good quality.

V. Results and Discussion

A. Inversion Success of MSG and MODIS BRDF

The BRDF model produced using MSG data as an input contains substantially more full inversions than the corresponding MODIS data, particularly in regions that experience frequent cloud cover. This remains true even when comparing the 16-day MODIS product to daily MSG BRDFs.

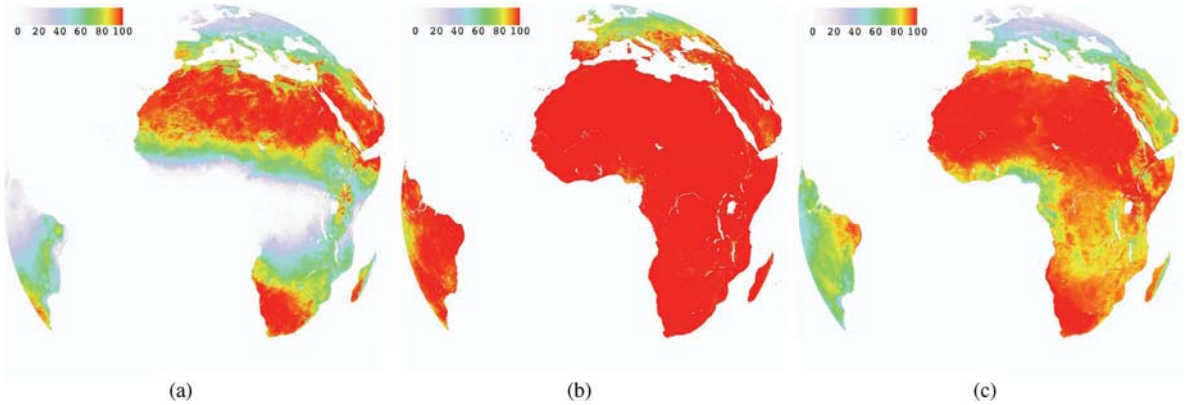

Fig. 1. Number of successful BRDF inversions during 2008 as a percentage of the total possible inversions. (a) MODIS 16-day BRDF. (b) MSG 16-day BRDF. (c) MSG daily BRDF.

Fig. 1 shows the percentage of successful BRDF inversions for MODIS and MSG for 2008. When examining the MODIS success rate, shown in Fig. 1(a), it is noticeable that, in central Africa, the 16-day data rarely result in a successful full inversion. A large number of pixels (covering approximately 2.8 Mkm^2) have no full inversions performed within the entire one-year period. A similar pattern is shown in other cloud-prone areas such as Madagascar, South America, and Scandinavia. The Sahara, being predominantly cloud free, has almost 100% of 16-day periods produce a successful full inversion for MODIS. A similar map is shown for the 16-day MSG average in Fig. 1(b). For Africa, it is clear that a much larger number of pixels experience high percentages of successful inversions, particularly in the cloud-prone central areas in which MODIS is unable to produce many inversions. Areas of central Africa that, with MODIS, allowed only 0%–10% of the retrievals to be successfully inverted show a success rate of greater than 80% with the MSG 16-day data. Cloud-free areas show little difference to MODIS, with almost 100% of retrieval periods producing a successful inversion. Outside of Africa, the MSG 16-day data also show a higher success rate than MODIS: For South America, the success rate increases from 10%–20% with MODIS to 80%–90% with MSG. Europe is similar, and MSG shows a success rate that is around 20% higher than that of MODIS. It can be seen from Fig. 1(b) that cloud cover is not the dominant factor in determining the success of the MSG BRDF on a 16-day timescale. Instead the VZA appears more important: Pixels with a high VZA show a lower percentage of successful BRDF inversions.

The BRDF success is partially defined by its ability to normalize reflectances to the modeled case of the sensor being nadir to the pixel. For areas with low VZA, this requires little extrapolation between the actual and modeled reflectances, but for areas with high VZAs, there are no input observations that can be used to constrain the BRDF, and hence, it can become unstable. This can be partially overcome by the reciprocity between VZA and SZA, allowing observations with a low SZA (e.g., near midday) to be used in place of observations with low VZA. However, in some cases, the SZA is also high, particularly for Europe during the winter months, and therefore, there will be no observations with either low VZA or SZA. This explains why areas like Scandinavia with both high VZA and latitude show a lower success rate than areas with a similar VZA but much lower latitude such as South America. Unfortunately, this is a limitation of geostationary data that cannot be overcome without adding an additional data source, such as a polar-orbiting sensor that is able to provide low VZA views at high latitudes.

TABLE I
MEAN AND STANDARD DEVIATION OF MSG–MODIS DIFFERENCES FOR THE CHANNELS 1, 2, AND 3 AVERAGED OVER 2008. THE ABSOLUTE DIFFERENCES ARE (MSG-MOD), AND THE RELATIVE DIFFERENCES ARE (MSG-MOD)/[0.5 ∗ (MSG + MOD)]

Channel		Absolute Diff.	Relative Diff.	RMSE
Channel 1 ($0.6\mu m$)	μ	0.020	0.152	0023
	σ	0.013	0.122	0.015
Channel 2 ($0.8\mu m$)	μ	0.037	0.126	0.045
	σ	0.020	0.086	0.021
Channel 3 ($1.6\mu m$)	μ	0.029	0.098	0.054
	σ	0.020	0.087	0.023

Fig. 1(c) shows the success rate of the shorter timescale daily MSG retrievals. These still show an improved success rate over the MODIS data in many areas, with central Africa now producing a full inversion for around 50% of retrievals. Although the probability of a successful inversion is higher in Africa and South America for MSG than MODIS, the same is not true in Europe. At the daily timescale, cloud cover becomes important, so for Europe, the combination of high VZA and a low number of cloud-free observations means that the BRDF likelihood of a successful inversion on any one day is relatively low.

Overall, this section highlights the advantage of SEVIRI's high temporal resolution. MSG provides at least 20 times as many looks at a given area per day than MODIS, and this leads to a much higher probability of being able to characterize the land surface accurately enough to produce a full BRDF inversion. Even on the daily timescale, MSG displays an improvement over the 16-day MODIS retrieval, enabling MSG-BRDF data to be used in examining short-term and rapidly developing phenomena such as fire, flooding, droughts, and the onset of the rainy season. On average, the daily MSG retrieval is successful for 81% of pixels, the 16-day MSG retrieval is

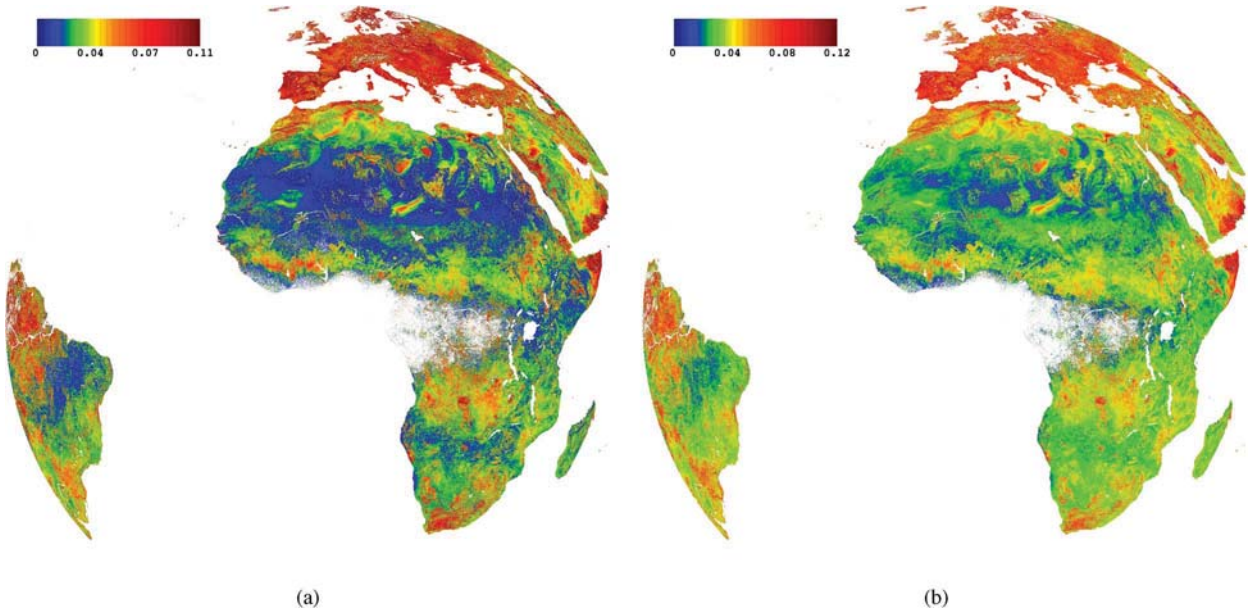

Fig. 2. Differences between MSG and MODIS 0.8-μm reflectances averaged over all acquisitions in 2008. Central Africa and some parts of Western Africa are not shown due to a lack of full inversions in the MODIS BRDF product. (a) Absolute difference (MSG-MOD). (b) RMSE.

successful for 92% of pixels, and the MODIS 16-day retrieval is successful for around 62% of pixels. Since MODIS employs a backup inversion method, the actual number of pixels with NBAR reflectances within the MODIS products is higher than shown here, as only full inversions are considered. These NBAR values produced by the backup inversion are typically of lower accuracy than those produced with the full inversion, however. This is particularly true in times of rapid land surface change when the historical database of BRDF values used by the backup method may not match the true state of the land surface.

It is also important to examine the quality of the MSG-BRDF data. The fixed viewing geometry of MSG severely limits the angular sampling of the surface bidirectional reflectance response, particularly in the cross principal plane for which the variance of the surface anisotropy is limited. The following sections explore the accuracy of the MSG-BRDF data relative to MODIS and *in situ* data.

B. Comparison of MODIS and MSG for the Whole Scene

The RMSE and absolute and relative differences between MSG and MODIS are summarized in Table I for all three VNIR channels while Fig. 2 shows the absolute difference and RMSE for Channel 2 across the full disk. These data indicate that there is generally a good match between the two BRDF methods, particularly as the MODIS algorithm was designed to keep the uncertainty to below 10% in most conditions. Although the mean difference is higher than 10% for channels 1 and 2, this is partially due to the slight differences in spectral bandwidth between SEVIRI and MODIS, meaning that, even if the BRDF model functioned perfectly, there would still be differences between the two sets of reflectances. This is exacerbated for channel 1 as, for much of the disk, the reflectances in this channel are low, thereby meaning that a small uncertainty in the reflectance translates into a much larger relative difference than for channels 2 or 3. The BRDF algorithm flags pixels as good quality if the RMSE between the BRDF model and the observed reflectances is less than 0.1, and if a similar criterion is used to define the success of the MSG BRDF compared to MODIS, the results are very promising: Averaged over all three channels, 98.3% of pixels return an RMSE that is less than 0.1. For the remaining 1.7% of reflectance observations that are of high RMSE, the mean VZA is 68°, and 61.9% of these pixels are located at a VZA greater than 65°, the maximum VZA for which the SMAC atmospheric correction algorithm is accurate [40]. Across most of the scene, the MSG reflectances are lower than those of MODIS, but in areas where the VZA is larger (such as the extremes of South America and Northern Europe), it is the MSG NBARs that are higher. This could be due to the BRDF model attempting to fit poor quality data in these cases, as it is attempting to normalize the VZA to 0°, which introduces errors in cases where no low solar or viewing zenith angle observations were made. When the sun is far from the pixel location (such as during the local winter time), neither the solar nor viewing angle would be low—thus decreasing the quality of the BRDF model. Furthermore, as described in [40], the accuracy of the atmospheric correction method used upon the MSG data decreases with increasing zenith angle, so at the very high VZAs, there will be an artificial increase in the reflectance values used as an input to the MSG-BRDF code. Due to the differing correction method applied to the MODIS data and due to the varying viewing geometry associated with MODIS, this will be less of a problem for that instrument. Additionally, in the area directly to the North of the MSG sensor, which lies in the cross principal plane, the MSG reflectances are higher than that of MODIS. Most of the reflectance anisotropy is contained in the principal plane, while the cross principal plane contains the least variance in reflectance. This means that a modeled BRDF in the cross principal plane is more sensitive to uncertainty in the input reflectances than one from outside this region. However, close to the subsatellite point, within the

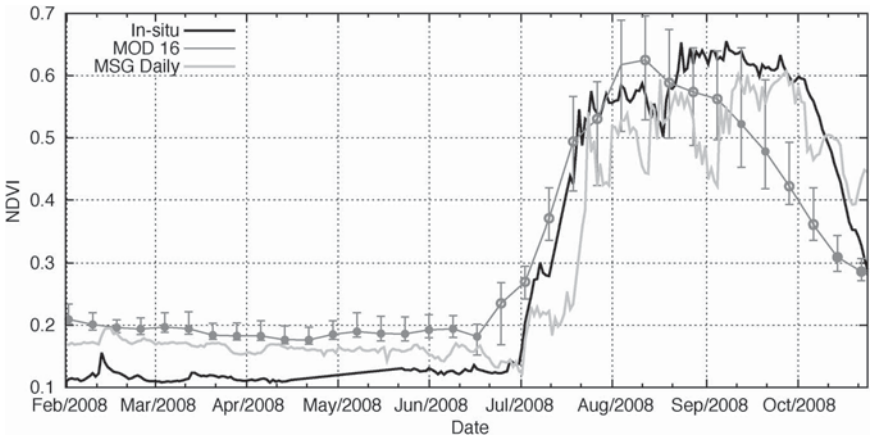

Fig. 3. MODIS 16-day and MSG daily BRDF NDVIs plotted alongside *in situ* data at the Dahra field site in Senegal for 2008. For the MODIS 16-day BRDF, the closed circles represent a full inversion by the BRDF model, and the open circles denote a magnitude, or backup, inversion. The error bars represent the minimum and maximum NDVI values across all the MODIS pixels contained within the SEVIRI pixel that covers Dahra.

cross principal plane, the VZA is low—meaning that it is still possible to produce good NBARs. Further to the North, the VZA increases while the cross principal plane is still limiting the angular sampling, and this means that the BRDF model is less suited to producing NBARs, as no low zenith angle data are available. This explains why both the absolute difference and the RMSE are higher in Europe than for areas with a similar VZA in South America or Arabia.

Despite the generally good match between MSG and MODIS reflectances, there are a number of areas in which the MSG–MODIS difference is high. Most notable are the regions of central Africa that, as shown in Fig. 1(c), experience the lowest number of successful inversions. In this area, the relative difference is typically around 15%–20%, but for some pixels, it can be greater than 25%. This is most likely a result of persistent cloud cover in the region that reduces the possibility of gaining clear-sky reflectance observations as a BRDF input. The high relative difference in the cloud-prone regions is due to numerous reasons. First, the MODIS correction method is not always completely successful in removing residual cloud or thick atmospheres. Second and more significantly, there are times when the MSG-BRDF results are corrupted by the inclusion of cloud-contaminated reflectances. If such reflectances are included, then there will be a large deviation in MSG reflectances compared to the actual, and MODIS, reflectances—thereby resulting in a high relative difference. In areas where cloudiness is less of a problem, such as the Sahel, Sahara, and South Africa, the relative difference between sensors is much lower, typically between 0% and 5%. Some of the high peaks in the Sahara do display a variation in difference, as does the region directly to the North of the sensor, in the cross principal plane.

For much of the full disk, the MSG-BRDF method shows low relative difference to MODIS, meaning that a large degree of confidence can be placed in the results generated by MSG BRDF. However, in areas where cloudy conditions are a frequent occurrence, care must be taken with the inclusion of cloud-contaminated reflectances into the BRDF inversion as this produces a substantial increase in the relative difference between MSG and MODIS. Additionally, the relative difference increases for high VZAs, meaning that less confidence can be placed in the results retrieved in pixels far from nadir.

C. Comparison With Field Site Data

The evolution of the MODIS and MSG BRDF-derived NDVIs throughout 2008 is shown for the Dahra field site in Fig. 3. This shows the *in situ* data on a daily basis, the MSG data on a daily timescale, and the MODIS data on overlapping 16-day acquisition periods. Data that are produced as a result of a full MODIS inversion are shown as filled while those that result from a magnitude inversion are open circles. It is immediately noticeable that there is a significant difference between the MODIS/MSG data and the *in situ* data for the dry season, running until mid-June. This difference is due to the small scale ploughing work that was carried out at the field site location, meaning that more bare soil is visible for the *in situ* sensors than for the large-area satellite sensors. However, the MODIS and MSG data produce similar values throughout this time period, with MODIS NDVIs being slightly lower than those from MSG, and this is due to differences in the spectral bands used by the sensors. The MSG data display a greater amount of variation than MODIS, and this is due to two factors: First, the shorter compositing time used in the MSG data series means that short-term variations in the land surface are more likely to be picked up than in the MODIS data. An example of this is in mid-February when a sudden rain shower briefly increased the NDVI due to the darkening of the soil. This is visible in the *in situ* data as a sharp NDVI peak and is also visible, to a lesser extent, in the MSG data series. It is not, however, visible within the MODIS results due to the much longer retrieval period of these data, and a short deviation such as this would be ignored as an outlier.

Second, some of the variation cannot be attributed to actual changes in the land surface but are a result of errors within the MSG-BRDF processing. The MODIS data use much stricter criteria for the selection of valid input data than MSG, with some scenes being removed due to cloud contamination, aerosol content, or poor scene geometry. MSG, on the other hand, allows many more observations to be used—even if they

may be of lower quality. This results in some of the input observations containing reflectance values that are not representative of the land surface being examined. A further issue is that the Dahra pixel lies close to the cross principal plane, perpendicular to the path of the sun, in which the surface reflectance is least sensitive to angular variation. As a result of this, the inversion is somewhat unstable at times of year when the sun is at a similar latitude as the pixel, and the values that are output may be of lower quality than at other times of year. This is noticeable in June as an increase in the variability of the NDVI data produced by MSG. During the wet season, both MODIS and MSG data follow the increase in NDVI shown by the field data, although MODIS uses only the magnitude inversion due to a lack of sufficient input reflectances. During the latter stages of the rainy season (August and September), both MODIS and MSG underestimate the NDVI when compared to the field site, a problem that is worse for the MODIS data than MSG. MODIS underestimates by up to 0.15 while MSG underestimates the NDVI by up to 0.1 NDVI units. Throughout the entire rainy season, there is substantially more variability in the MSG data series than is visible for the corresponding MODIS data. This is partially due to much of the MODIS data being based on the magnitude inversion, which is inherently smoother than a full BRDF inversion as it relies on a backup BRDF parameter database. Even so, the MSG variance is high, indicating that, as stated earlier, some of the reflectance data that have been included in the BRDF inversion were not suitable. It may be possible to reduce this variance by applying stricter acceptance criteria to the MSG data series or by excluding poor full inversion results by using stricter WoD criteria upon the results of the inversion. However, in its current state, the MSG-BRDF algorithm relies only upon the full inversion, not the magnitude inversion, and is thus unable to compute NBARs in cases when the full inversion fails. That said, the error bars associated with the MODIS data indicate that, across all MODIS pixels within the larger SEVIRI pixel, there is considerable variability—up to 20% or 0.12 NDVI units. We believe that this is due to residual cloud contamination and poor BRDF fitting within the MODIS product, as the land surface around Dahra is homogeneous enough so that it should not display such large variations over a relatively small spatial extent. Overall, this comparison has shown that, in many circumstances, the MSG nadir-corrected NDVI can accurately describe the surface conditions and corresponds well to the equivalent data derived from MODIS in cloud-free conditions. The smaller acquisition time associated with MSG means that additional variation in the NDVI curve is noticeable in the MSG data, both describing real surface effects and errors due to the contamination of the input reflectances. However, under some conditions, the MSG data are of very low quality, with high intraperiod variation and large differences to the expected NDVI. This can primarily be attributed to many unsuitable reflectances being used to generate the BRDF products. By tightening the criteria for the selection of suitable input reflectances and through the use of a more accurate cloud mask, this problem can be reduced, and by the inclusion of a magnitude inversion of the same type as used by MODIS, this problem may be totally avoided. Stricter use of WoD criteria would result in fewer full inversions being performed by MSG, but the magnitude inversion could then be used instead, still allowing an accurate NBAR data series to be produced without the variance noted in many of the wet season MSG data points.

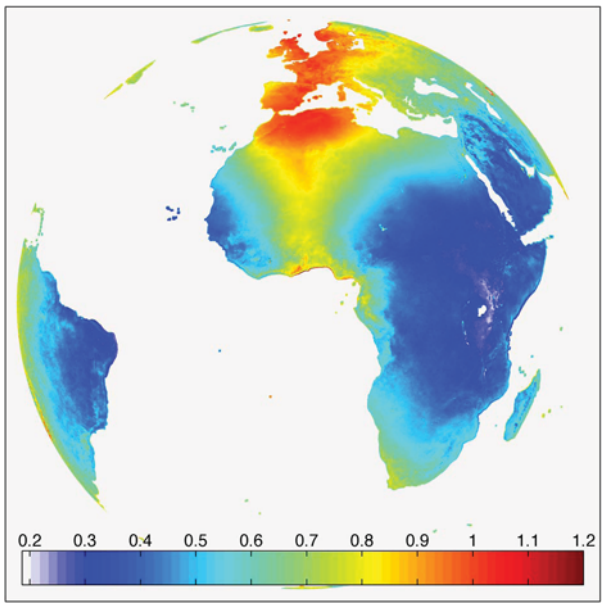

Fig. 4. Spatial distribution of the weights of distribution in the Nadir45 case averaged over 2008.

D. WoD

The WoDs are an important parameter in assessing the quality of the BRDF model that is produced by the MSG algorithm. This section focuses upon the WoDs produced with a simulated 45° SZA and 0° VZA, known as Nadir45, that were produced during 2008 in order to assess the MSG NBAR reflectances for the African continent. For this section, the BRDF algorithm was modified in order to remove the MODIS WoD thresholds, as this enables all full inversions to be flagged as good and thus saves the WoD values, regardless of their quality. The White Sky Albedo WoDs were also produced but are not investigated in detail here as they display a very similar pattern of results to the Nadir45 WoDs.

The results of the MSG Ch01 WoDNadir case are shown in Fig. 4, and it is clear that, for the majority of the scene, the WoDs are low, much lower than the MODIS cutoff figure of 1.25. However, areas with higher VZAs typically show much higher WoDs, with VZAs of 60° exhibiting WoDs that are, on average, twice as high as those recorded at a VZA of 15°. This functional dependence of the WoD Nadir45 upon VZA is shown in Fig. 5(a). There is a large spread of values due to the changing surface conditions, azimuth angles, and input observations, but an increasing trend of WoD upon VZA is noticeable. There is also a region in the Sahara and Morocco where the WoDs are much higher than in the surroundings. This region is centered upon 0° longitude and is where the pixel is near the cross principal plane to the sun. The majority of BRDF information is contained in the principal plane, that in which the sun moves. If the Relative Azimuth Angle between the sensor and sun at a particular pixel is always close to either

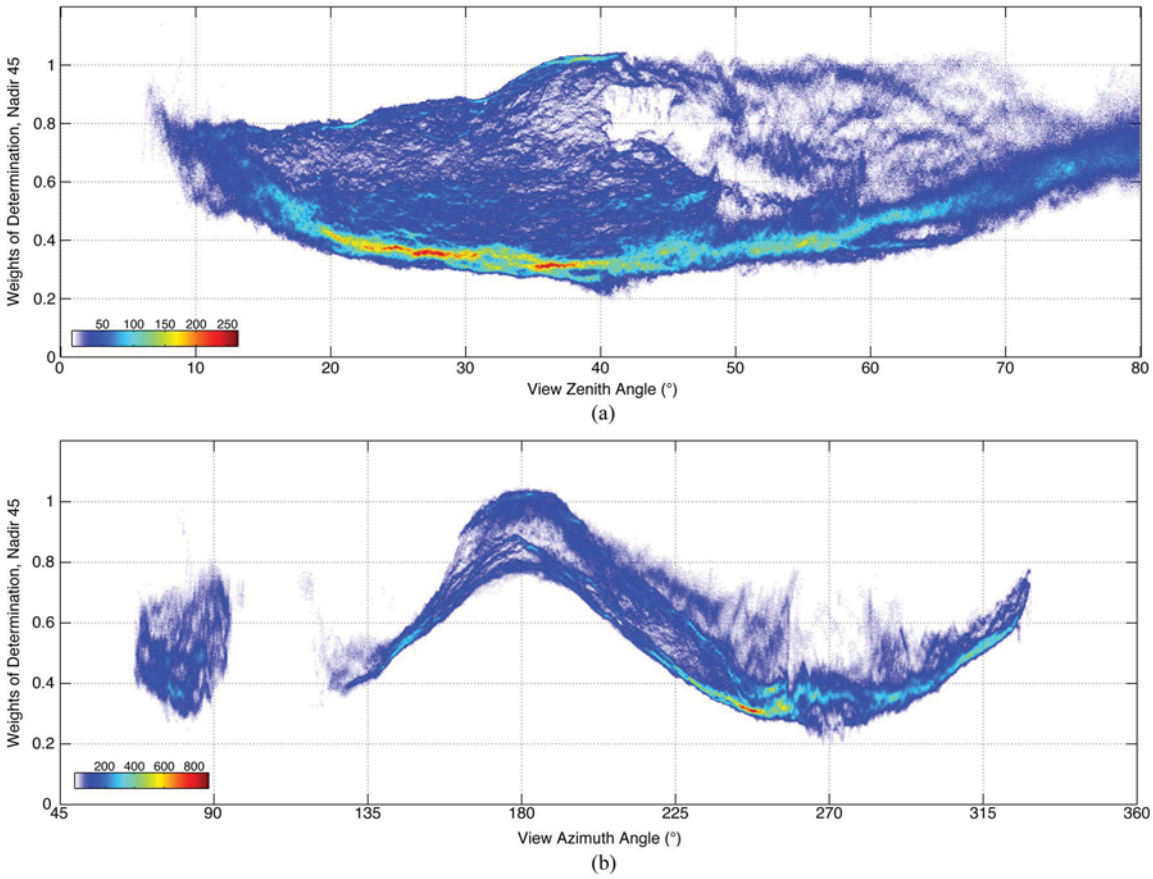

Fig. 5. Effects of view zenith and azimuth angles upon the Nadir 45 WoDs. The color scale indicates the number of pixels in the full MSG disk that fall into a particular angle/WoD bin. (a) Plot of average NWoDs in 2008 against the MSG VZA. (b) Plot of average NWoDs in 2008 against the MSG VAA.

90° or 270°, then much of the BRDF information is lost, and the quality of inversion is therefore reduced. A plot of WoDN45 against VAA, as shown in Fig. 5(b), highlights this issue. A peak in the WoDs is visible at a VAA of 180°, corresponding to the 0° longitude region. As the VAA moves away from 180°, the WoDs decrease rapidly. This is due to the cross principal plane problem, evident in Fig. 4, and is a regional problem specific to satellites that have a fixed viewing geometry. Despite these problems in the cross principal plane and at high VZAs, the majority of the four-day retrieval provides good reflectance data in this case, including the cloud-prone central Africa region.

For the pixels that show the worst NBAR reflectances, the WoDs are high, higher than the MODIS threshold, but even for many pixels that produce NBAR reflectances that are close to what is expected, the WoDs can still be high, particularly in the subsatellite zone. This means that applying the MODIS thresholds directly to the MSG data as a method of quality control is not feasible, as BRDF retrievals that are good enough to generate an NBAR may be rejected within the algorithm due to the high WoD values. A new set of WoD thresholds must be produced that are both specific to the SEVIRI data set and tailored to the required output.

When examining a single retrieval rather than a yearly average, there are numerous pixels that do display a WoD that is higher than the acceptable MODIS threshold. Primarily, these occur in the cloud-prone central African region and are also noticeable at high VZAs in Madagascar and the Arabian peninsula. These high values are variable, however, and strongly depend upon the number of good-quality clear-sky observations of the land surface that are available within any one acquisition period. This is highlighted in Fig. 1(c): The majority of pixels that did not gain a BRDF retrieval failed due to WoD or RMSE values being too high rather than because cloud cover meant a complete lack of input data. Typically, the cloud cover would reduce the number of usable input observations, and then, WoD or RMSE thresholds would declare the retrieved BRDF to be bad. This may be due to undetected cloud contamination or—particularly in the case of Europe—because the combination of having only a few input observations and high VZA/SZAs means that the resulting BRDF will be of poor quality. Indeed, during European wintertime, there are many more failed retrieval, an average of 370 000, than in summertime where the average is around 150 000. This is likely due to both the higher number of clear-sky observations over Europe in summertime and (because the sun is North of the equator) the lower SZAs for European pixels compared to wintertime. Over the whole of 2008, there are an average of 1.8% of pixels per retrieval that fail due to the WoD/RMSE quality checks. The highest percentage of failed inversions occurs on December 6 (3.31%) while the lowest occurs on July 4 (0.87%). The RMSE test fails the largest number of pixels (an average of 1.4% per retrieval) while the weights of determination for white sky albedo (WoDWSA) and WoDN45 tests fail a significantly lower number of pixels (0.48% and 0.04%, respectively). The

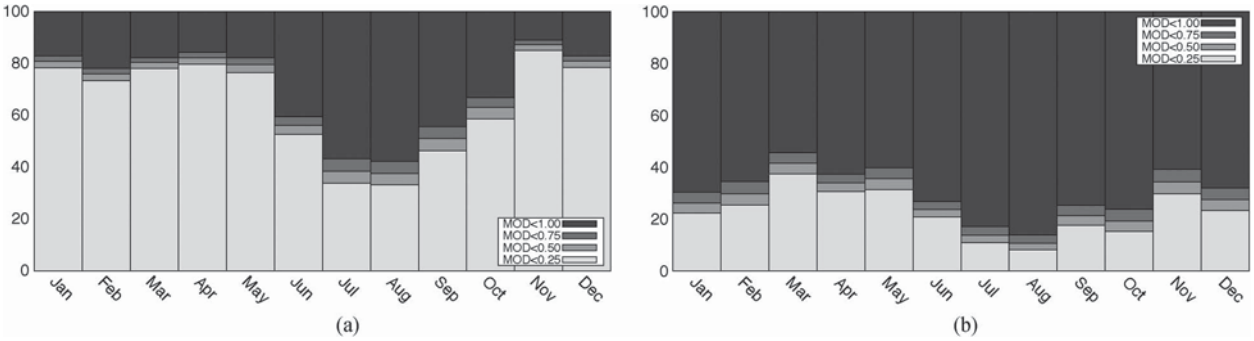

Fig. 6. Comparisons of the MSG and MODIS cloud masks for the cloud-free and cloud-filled cases in each month of 2008 for the West African tile (h16v07). For the MODIS data, the values are divided into categories in which less than 25%, 50%, 75%, or 100% of MODIS pixels within the MSG pixel are marked as cloud free. (a) Pixels marked as cloud free by MSG. (b) Pixels marked as cloud contaminated by MSG.

WoDN45 test remains fairly constant throughout the year in terms of the number of pixel failures while WoDWSA fails approximately 35% more pixels during February and October than in any other months. We are unsure as to why this is, but it appears to be related to scene geometry rather than to cloud contamination. The RMSE tests show the largest seasonal variation in pixel failure—three times as many pixels fail the RSME tests in January and December than in June and July.

In order to resolve the issue of higher WoD values in the cross principal plane, additional data are required as an input. This could take the form of data from other instruments, such as MODIS, advanced very high resolution radiometer, or others, but then, problems arise in normalizing the different spectral bands between sensors. Additionally, because such sensors are polar orbiting, they will only have one or two overpasses per day. In cloud-prone regions, this means that it is possible that, within the window used to generate the MSG BRDF, there will be no cloud-free looks at the land surface by these other sensors, necessitating an increased acquisition period. This removes a large advantage of using the MSG platform in the first place—temporal resolution, as was successfully demonstrated with the original Meteosat system [61], [62]. Another solution could be to employ another SEVIRI sensor at a differing orbital longitude. As of 2013, there are two MSGs in operation, and the data used within this study are gathered from the MSG-2 platform at 0°E longitude (it has subsequently moved to 9.5°E), but MSG-1 was in operation at a longitude of 9.5°E. However, this platform operated in "rapid scan" mode and focuses only on Europe. One more MSG satellite is planned for launch though, and it is possible that, if MSG-1 and -2 are still operational, there may be more than one satellite gathering full-scene images for Africa at the same time—significantly improving the angular sampling input for the MSG-BRDF algorithm.

VI. Effects of Subpixel Cloud Contamination

The relatively large spatial footprint of each SEVIRI pixel means that subpixel clouds can be an issue, particularly in high-VZA regions where the pixel footprint is even larger. Even if a cloud covers a smaller area than an entire SEVIRI pixel, it can still affect the observed reflectance of that pixel and can therefore also have an effect upon the modeled BRDF. This section seeks to explore the effectiveness of the MSG cloud mask in detecting subpixel clouds through a comparison to the 1-km MODIS cloud mask. The comparison takes place across two MODIS tiles: h16v07 that covers West Africa (including the Dahra field site) and h18v03 that covers Southern Scandinavia. The first tile is interesting as it enables an analysis for Dahra that, as has been shown in Section V-C, is likely to be heavily affected by cloud contamination during the wet season. The second tile contrasts this by analyzing an area with a much larger pixel footprint (approximately 6.5 km North–South and 3.5 km East–West) and hence is thought to be more prone to subpixel clouds. To perform the comparison, the MODIS cloud mask was extracted from the MOD09GA product at a 1-km resolution for both tiles. The corresponding SEVIRI data were extracted based upon the solar azimuth angle of the MODIS data (as it provides an estimate of the overpass time, and hence which SEVIRI 15-min images to use). Each SEVIRI pixel contains 12–15 MODIS pixels in West Africa and 40–50 pixels in Scandinavia. For both satellites, all pixels flagged as either cloud filled or cloud contaminated were marked as cloudy. For the MODIS data, an average was made to give a value between 0 and 1 that indicates the proportion of MODIS pixels within each SEVIRI pixel that were marked as cloudy. The results were split into two categories for each tile: one that compares pixels marked as cloud free by SEVIRI to the associated MODIS proportion and one that compares pixels marked as cloud filled to MODIS.

Fig. 6 shows the results of this comparison for West Africa. The MSG cloud mask appears to let through large amounts of cloud-contaminated pixels [see Fig. 6(a)]. For pixels flagged as cloud free by MSG, an average of 35% are flagged by MODIS as containing a proportion of more than 0.25 cloud cover. The situation is particularly bad between June and September as, for these months, more than 66% of MSG pixels noted as clear are flagged as cloud contaminated by MODIS. These "cloud-free" pixels are ingested into the BRDF algorithm and will reduce the quality of the final retrieval. This may well explain a lot of the uncertainty present in Fig. 3, particularly during the wet season. The MSG cloud mask also appears too conservative in some cases [see Fig. 6(b)], with 22% of all pixels flagged as cloudy by MSG showing a proportion of less than 0.25 cloud cover in the MODIS cloud mask. For several months of the year, this increased to more than 30% of pixels—meaning that a large number of MSG pixels are flagged as cloudy even though they

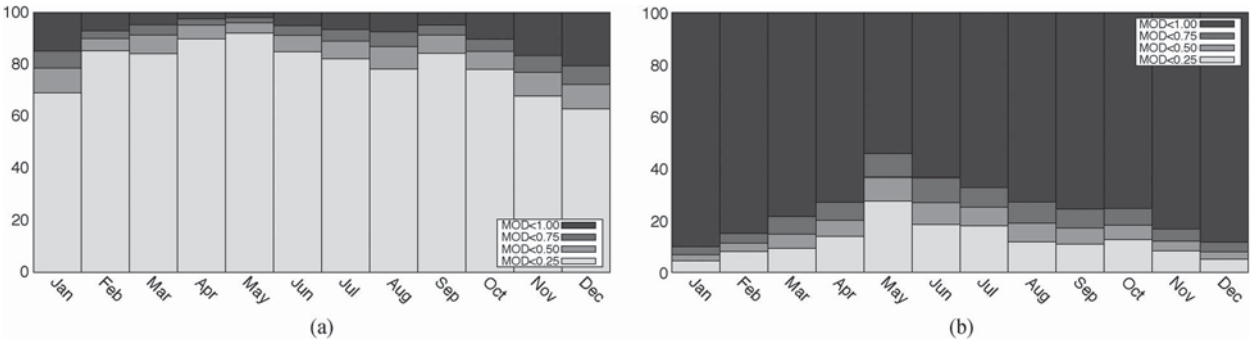

Fig. 7. Comparisons of the MSG and MODIS cloud masks for the cloud-free and cloud-filled cases in each month of 2008 for the Scandinavian tile (h18v03). For the MODIS data, the values are divided into categories in which less than 25%, 50%, 75%, or 100% of MODIS pixels within the MSG pixel are marked as cloud free. (a) Pixels marked as cloud free by MSG. (b) Pixels marked as cloud contaminated by MSG.

may actually give usable reflectances. The comparison for the Scandinavian region is shown in Fig. 7. The results here are more encouraging: For pixels marked as cloud free by SEVIRI [see Fig. 7(a)], an average of 80% have a proportion of less than 0.25 MODIS pixels flagged as cloudy, while for pixels marked as cloudy by SEVIRI [see Fig. 7(a)], an average of 87% are also flagged as cloudy by MODIS. In terms of falsely flagging pixels as cloudy, the MSG cloud mask performs worst in December and January where only 65% of pixels are flagged as clear by MODIS. This may well be due to the SEVIRI cloud masks relying heavily upon reflectance data to determine the cloud state. In the winter months, the low solar zenith angle precludes this approach for much of Northern Europe, and the cloud state must be determined from the thermal bands only. Taken jointly, the studies at these two sites indicate that there are flaws in the SEVIRI cloud mask methods that can allow contaminated pixels into the BRDF processing chain. There are also signs that the SEVIRI cloud mask excludes pixels unnecessarily, meaning that fewer observations of the land surface are available than are possible. Both of these factors will reduce the accuracy of BRDF retrievals for affected pixels.

VII. Conclusion and Perspectives

This paper has shown that the application of the MODIS DB BRDF model to SEVIRI geostationary reflectances is successful. The MODIS BRDF model was applied with a daily retrieval period, resulting in a substantial increase in temporal resolution compared to the MODIS 16-day BRDF retrievals. These daily MSG retrievals do not require additional input, unlike the Land-SAF BRDF products that use multiple satellites. A comparison to MODIS data showed that, in many circumstances, the MSG data are of high quality and can produce accurate reflectance values for much of the full SEVIRI disk. However, several areas exist in which the MODIS and MSG BRDF-adjusted data differ substantially. These pixels are situated either at high VZAs or in cloud-prone areas. A comparison between both MSG and MODIS data to that gathered by ground-based sensors in Dahra, Senegal, showed that both display differences to the *in situ* data. In the case of the MSG data, this is primarily due to cloud contamination within the input data series which could be resolved by the application of a more accurate cloud mask coupled to stricter criteria within the BRDF method on which input reflectances are to be used in performing the BRDF inversion. Despite these uncertainties, the MSG method is successful at producing BRDF-adjusted reflectances in such cloud-prone areas. In central Africa, the MSG-BRDF model is up to 100 times more likely to produce a successful inversion than MODIS within a given 16-day period. Even if the MSG selection criteria are redefined more strictly, the MSG-BRDF method will still produce significantly more successful inversions than MODIS for these cloud-prone regions.

When examining the internal WoD used by the BRDF model to assess the quality of inversion, there are several areas of the MSG scene in which the inversion quality is reduced. These typically occur at high VZAs or in the cross principal plane (equating to a VAA of 180°). The cross principal plane problem is inherent in geostationary data due to the fixed viewing geometry as, in this plane, there is a severe reduction in reflectance variation due to surface anisotropy. This reduction means that the BRDF fit in this plane is less stable than in other regions, such as within the principal plane itself, so the quality of fit is reduced. This problem is hard to overcome and will rely on the addition of other data gathered under a different set of viewing geometry. Such data could be acquired from polar-orbiting sensors or from another geostationary sensor located at a different longitude. Outside of the cross principal plane and at low VZAs (under 65°), the quality of inversion by the MSG-BRDF model is found to be high, and if a suitable cloud mask is applied, data produced by this method can therefore be used with confidence.

Acknowledgment

Part of this work was carried out while S. R. Proud was a visiting scientist at the Center for Remote Sensing, Boston University. C. Schaaf, M. Friedl, and M. Holmes are thanked for making this visit possible as well as for their hospitality and assistance in Boston. Q. Zhang is thanked for his advice and expertise with the MODIS algorithms while Y. Shuai is also thanked for her assistance in compiling and running the MODIS direct-broadcast bidirectional-reflectance-distribution-function code. C. Schaaf and Q. Zhang were supported under NASA grants NNX08AE94A and NNG04GP09G. The authors would like to thank the anonymous reviewers for their very useful thoughts and ideas on this manuscript.

REFERENCES

[1] B. Brennan and W. R. Bandeen, "Anisotropic reflectance characteristics of natural earth surfaces," *Appl. Opt.*, vol. 9, no. 2, pp. 405–412, Feb. 1970.

[2] D. Kimes and P. Sellers, "Inferring hemispherical reflectance of the earth's surface for global energy budgets from remotely sensed nadir or directional radiance values," *Remote Sens. Environ.*, vol. 18, no. 3, pp. 205–223, Dec. 1985.

[3] F. E. Nicodemus, "Directional reflectance and emissivity of an opaque surface," *Appl. Opt.*, vol. 4, no. 7, pp. 767–773, Jul. 1965.

[4] C. Schaaf, F. Gao, A. Strahler, W. Lucht, X. Li, T. Tsang, N. Strugnell, X. Zhang, Y. Jin, J. Muller, P. Lewis, M. Barnsley, P. Hobson, M. Disney, G. Roberts, M. Dunderdale, C. Doll, R. d'Entremont, B. Hu, S. Liang, J. L. Privette, and D. Roy, "First operational BRDF, albedo nadir reflectance products from MODIS," *Remote Sens. Environ.*, vol. 83, no. 1, pp. 135–148, Nov. 2002.

[5] O. Pokrovsky and J.-L. Roujean, "Land surface albedo retrieval via kernel-based BRDF modeling: I. Statistical inversion method and model comparison," *Remote Sens. Environ.*, vol. 84, no. 1, pp. 100–119, Jan. 2003.

[6] O. Pokrovsky and J.-L. Roujean, "Land surface albedo retrieval via kernel-based BRDF modeling: II. An optimal design scheme for the angular sampling," *Remote Sens. Environ.*, vol. 84, no. 1, pp. 120–142, 2003.

[7] J. Roujean, M. Leroy, and P. Deschanps, "A bidirectional reflectance model of the Earth's surface for the correction of remote sensing data," *J. Geophys. Res.*, vol. 97, no. D18, pp. 20 455–20 468, Dec. 1992.

[8] W. Wanner, X. Li, and A. Strahler, "On the derivation of kernel-driven models of bidirectional reflectance," *J. Geophys. Res.*, vol. 100, no. D10, pp. 21 077–21 090, Oct. 1995.

[9] W. Lucht, C. Schaaf, and A. Strahler, "An algorithm for the retrieval of albedo from space using semiempirical BRDF models," *IEEE Trans. Geosci. Remote Sens.*, vol. 38, no. 2, pp. 977–998, Mar. 2000.

[10] C. L. Walthall, J. M. Norman, J. M. Welles, G. Campbell, and B. L. Blad, "Simple equation to approximate the bidirectional reflectance from vegetative canopies and bare soil surfaces," *Appl. Opt.*, vol. 24, no. 3, pp. 383–387, Feb. 1985.

[11] M. Minnaert, "The reciprocity principle in lunar photometry," *Astrophys. J.*, vol. 93, no. 3, pp. 403–410, May 1941.

[12] H. Rahman, B. Pinty, and M. Verstraete, "Coupled surface-atmosphere reflectance (CSAR) model. II: Semiempirical surface model usable with NOAA Advanced Very High Resolution Radiometer data," *J. Geophys. Res.*, vol. 98, no. D11, pp. 20 791–20 801, Nov. 1993.

[13] O. Engelsen, B. Pinty, M. Verstraete, and J. Martonchik, "Parametric Bidirectional Reflectance Factor Models: Evaluation, Improvements and Applications, Report EUR16426EN," European Commission, Joint Research Centre, Space Applications Institute, Ispra, Italy, 1996.

[14] J. Martonchik, D. Diner, B. Pinty, M. Verstraete, R. Myneni, Y. Knyazikhin, and H. Gordon, "Determination of land and ocean reflective, radiative, and biophysical properties using multiangle imaging," *IEEE Trans. Geosci. Remote Sens.*, vol. 36, no. 4, pp. 1266–1281, Jul. 1998.

[15] A. Strahler, J. Muller, W. Lucht, C. Schaaf, T. Tsang, F. Gao, X. Li, P. Lewis, and M. Barnsley, "MODIS BRDF/albedo product: Algorithm theoretical basis document version 5.0," MODIS documentation 1999.

[16] J. Martonchik, D. Diner, R. Kahn, T. Ackerman, M. Verstraete, B. Pinty, and H. Gordon, "Techniques for the retrieval of aerosol properties over land and ocean using multiangle imaging," *IEEE Trans. Geosci. Remote Sens.*, vol. 36, no. 4, pp. 1212–1227, Jul. 1998.

[17] J. Martonchik, B. Pinty, and M. Verstraete, "Note on an improved model of surface BRDF-atmospheric coupled radiation," *IEEE Trans. Geosci. Remote Sens.*, vol. 40, no. 7, pp. 1637–1639, Jul. 2002.

[18] P. Deschamps, F. Bréon, M. Leroy, A. Podaire, A. Bricaud, J. Buriez, and G. Seze, "The POLDER mission: Instrument characteristics and scientific objectives," *IEEE Trans. Geosci. Remote Sens.*, vol. 32, no. 3, pp. 598–615, May 1994.

[19] F. Maignan, F. Bréon, and R. Lacaze, "Bidirectional reflectance of Earth targets: Evaluation of analytical models using a large set of spaceborne measurements with emphasis on the Hot Spot," *Remote Sens. Environ.*, vol. 90, no. 2, pp. 210–220, Mar. 2004.

[20] C. Bacour and F. Breon, "Variability of biome reflectance directional signatures as seen by POLDER," *Remote Sens. Environ.*, vol. 98, no. 1, pp. 80–95, Sep. 2005.

[21] F. Baret, O. Hagolle, B. Geiger, P. Bicheron, B. Miras, M. Huc, B. Berthelot, F. Nio, M. Weiss, O. Samain, J. L. Roujean, and M. Leroy, "LAI, fAPAR and fCover CYCLOPES global products derived from VEGETATION: Part 1: Principles of the algorithm," *Remote Sens. Environ.*, vol. 110, no. 3, pp. 275–286, Oct. 2007.

[22] B. Pinty, F. Roveda, M. Verstraete, N. Gobron, Y. Govaerts, J. Martonchik, D. Diner, and R. Kahn, "Surface albedo retrieval from Meteosat 1. Theory," *J. Geophys. Res.*, vol. 105, no. D14, p. 18099, Jul. 2000.

[23] B. Pinty, F. Roveda, M. M. Verstraete, N. Gobron, Y. Govaerts, J. V. Martonchik, D. J. Diner, and R. A. Kahn, "Surface albedo retrieval from Meteosat: 2. Applications," *J. Geophys. Res., Atmos. (1984–2012)*, vol. 105, no. D14, pp. 18 113–18 134, Jul. 2000.

[24] D. Carrer, J. Roujean, and C. Meurey, "Comparing operational MSG/SEVIRI land surface albedo products from Land SAF with ground measurements and MODIS," *IEEE Trans. Geosci. Remote Sens.*, vol. 48, no. 4, pp. 1714–1728, Apr. 2010.

[25] B. Geiger, D. Carrer, L. FranchistÉguy, J. Roujean, and C. Meurey, "Land surface albedo derived on a daily basis from Meteosat Second Generation observations," *IEEE Trans. Geosci. Remote Sens.*, vol. 46, pt. 2, no. 11, pp. 3841–3856, Nov. 2008.

[26] W. Lucht and P. Lewis, "Theoretical noise sensitivity of BRDF and albedo retrieval from the EOS-MODIS and MISR sensors with respect to angular sampling," *Int. J. Remote Sens.*, vol. 21, no. 1, pp. 81–98, 2000.

[27] B. Geiger, O. Hagolle, and P. Bicheron, "ATBD: Algorithm theoretical basis document, directional normalisation, cyclopes," CNRM, Toulouse, France, Tech. Rep., 2005.

[28] F. Gao, C. Schaaf, A. Strahler, Y. Jin, and X. Li, "Detecting vegetation structure using a kernel-based BRDF model," *Remote Sens. Environ.*, vol. 86, no. 2, pp. 198–205, Jul. 2003.

[29] D. Aminou, "MSG's SEVIRI instrument," *ESA Bulletin(0376-4265)*, no. 111, pp. 15–17, 2002.

[30] E. Cadau and G. Laneve, "Improved MSG-SEVIRI images cloud masking and evaluation of its impact on the fire detection methods," in *Proc. IGARSS*, 2008, vol. 2, pp. 1046–1059.

[31] J. Schmetz, P. Pili, S. Tjemkes, D. Just, J. Kerkmann, S. Rota, and A. Ratier, "An introduction to Meteosat Second Generation (MSG)," *Bull. Amer. Meteorol. Soc.*, vol. 83, no. 7, pp. 977–992, Jul. 2002.

[32] C. J. Tucker, "Red and photographic infrared linear combinations for monitoring vegetation," *Remote Sens. Environ.*, vol. 8, no. 2, pp. 127–150, May 1979.

[33] R. Fensholt, I. Sandholt, S. Stisen, and C. Tucker, "Analysing NDVI for the African continent using the geostationary Meteosat Second Generation SEVIRI sensor," *Remote Sens. Environ.*, vol. 101, no. 2, pp. 212–229, Mar. 2006.

[34] R. Fensholt and I. Sandholt, "Derivation of a shortwave infrared water stress index from MODIS near- and shortwave infrared data in a semi-arid environment," *Remote Sens. Environ.*, vol. 87, no. 1, pp. 111–121, Sep. 2003.

[35] J. Prieto, J. Epiphanio, L. Galvão, and L. Fonseca, "Global dissemination of meteorological information, EUMETCast or GEONETCast," in *Proc. Anais*, 2007, pp. 4159–4162.

[36] M. Derrien and H. Le Gléau, "MSG/SEVIRI cloud mask and type from SAFNWC," *Int. J. Remote Sens.*, vol. 26, no. 21, pp. 4707–4732, 2005.

[37] "Algorithm theoretical basis document for cloud products (cma-pge01 v3.2, ct-pge02 v2.2 & ctth-pge03 v2.2)," Satellite Applications Facility in Support to Nowcasting and Very Short Range Forecasting (NWC-SAF), Tech. Rep., 2012. [Online]. Available: http://www.nwcsaf.org/HTMLContributions/SUM/SAF-NWC-CDOP2-MFL-SCI-ATBD-1_v3.2.1.pdf

[38] H. Rahman and G. Dedeiu, "SMAC: A simplified method for the atmospheric correction of satellite measurements in the solar spectrum," *Int. J. Remote Sens.*, vol. 15, no. 1, pp. 123–143, 1994.

[39] S. R. Proud, R. Fensholt, M. O. Rasmussen, and I. Sandholt, "A comparison of the effectiveness of 6S and SMAC in correcting for atmospheric interference in Meteosat Second Generation images," *J. Geophys. Res., Atmos.*, vol. 115, no. D17, 2010.

[40] S. R. Proud, M. O. Rasmussen, R. Fensholt, I. Sandholt, C. Shisanya, W. Mutero, C. Mbow, and A. Anyamba, "Improving the SMAC atmospheric correction code by analysis of Meteosat Second Generation NDVI and surface reflectance data," *Remote Sens. Environ.*, vol. 114, no. 8, pp. 1687–1698, Aug. 2010.

[41] LPDAAC, Nadir BRDF-Adjusted Reflectance 16-day l3 0.05 deg cmg 2010 07. [Online]. Available: https://lpdaac.usgs.gov/lpdaac/products/modis_products_table/nadir_brdf_adjusted_reflectance/16_day_l3_0_05deg_cmg/mcd43c4

[42] E. Vermote, N. El Saleous, C. Justice, Y. Kaufman, J. Privette, L. Remer, J. Roger, and D. Tanré, "Atmospheric correction of visible to middle-infrared EOS-MODIS data over land surfaces: Background, operational

algorithm and validation," *J. Geophys. Res.*, vol. 102, no. 8, pp. 17 131–17 141, Jul. 1997.

[43] S. Kotchenova, E. Vermote, R. Matarrese, and F. Klemm, Jr., "Validation of a vector version of the 6S radiative transfer code for atmospheric correction of satellite data. Part I: Path radiance," *Appl. Opt.*, vol. 45, no. 26, pp. 6762–6774, Sep. 2006.

[44] S. Liang, H. Fang, M. Chen, C. Shuey, C. Walthall, C. Daughtry, J. Morisette, C. Schaaf, and A. Strahler, "Validating MODIS land surface reflectance and albedo products: Methods and preliminary results," *Remote Sens. Environ.*, vol. 83, no. 1, pp. 149–162, Nov. 2002.

[45] S. Liang, W. Lucht, Y. Jin, C. Schaaf, C. Woodcock, F. Gao, and X. Li, "Consistency of MODIS surface bidirectional reflectance distribution function and albedo retrievals: 2. Validation," *J. Geophys. Res.*, vol. 108, no. D15, p. 4159, Mar. 2003.

[46] J. Salomon, C. Schaaf, A. Strahler, F. Gao, and Y. Jin, "Validation of the MODIS bidirectional reflectance distribution function and albedo retrievals using combined observations from the aqua and terra platforms," *IEEE Trans. Geosci. Remote Sens.*, vol. 44, no. 6, pp. 1555–1565, Jun. 2006.

[47] L. Remer, J. Roger, and D. Tank, "Atmospheric correction of visible to middle-infrared EOS-MODIS data over land surfaces: Background, operational algorithm and validation," *J. Geophys. Res.*, vol. 102, no. D14, pp. 17131–17141, Jul. 1997.

[48] A. Huete, K. Didan, T. Miura, E. Rodriguez, X. Gao, and L. Ferreira, "Overview of the radiometric and biophysical performance of the MODIS vegetation indices," *Remote Sens. Environ.*, vol. 83, no. 1/2, pp. 195–213, Nov. 2002.

[49] Y. Jin, C. Schaaf, F. Gao, X. Li, A. Strahler, W. Lucht, and S. Liang, "Consistency of MODIS surface bidirectional reflectance distribution function and albedo retrievals: 1. Algorithm performance," *J. Geophys. Res.*, vol. 108, no. D5, p. 4158, Mar. 2003.

[50] J. Liu, C. Schaaf, A. Strahler, Z. Jiao, Y. Shuai, Q. Zhang, M. Roman, J. Augustine, and E. Dutton, "Validation of Moderate Resolution Imaging Spectroradiometer (MODIS) albedo retrieval algorithm: Dependence of albedo on solar zenith angle," *J. Geophys. Res.*, vol. 114, no. D1, pp. D01106-1–D01106-11, Jan. 2009.

[51] M. O. Romn, C. B. Schaaf, C. E. Woodcock, A. H. Strahler, X. Yang, R. H. Braswell, P. S. Curtis, K. J. Davis, D. Dragoni, M. L. Goulden, L. Gu, D. Y. Hollinger, T. E. Kolb, T. P. Meyers, J. W. Munger, J. L. Privette, A. D. Richardson, T. B. Wilson, and S. C. Wofsy, "The MODIS (collection v005) BRDF/albedo product: Assessment of spatial representativeness over forested landscapes," *Remote Sens. Environ.*, vol. 113, no. 11, pp. 2476–2498, Nov. 2009.

[52] M. Roman, C. Schaaf, P. Lewis, G. Feng, G. Anderson, J. Privette, A. Strahler, C. Woodcock, and M. Barnsley, "Assessing the coupling between surface albedo derived from MODIS and the fraction of diffuse skylight over spatially-characterized landscapes," *Remote Sens. Environ.*, vol. 114, no. 4, pp. 738–760, 2010.

[53] M. Lind, K. Rasmussen, H. Adriansen, and A. Ka, "Estimating vegetative productivity gradients around watering points in the rangelands of Northern Senegal based on NOAA AVHRR data," *Danish J. Geogr.*, vol. 103, no. 1, pp. 1–15, 2003.

[54] R. Fensholt and I. Sandholt, "Evaluation of MODIS and NOAA AVHRR vegetation indices with *in situ* measurements in a semi-arid environment," *Int. J. Remote Sens.*, vol. 26, no. 12, pp. 2561–2594, 2005.

[55] R. Fensholt, I. Sandholt, and S. Stisen, "Evaluating MODIS, SPOT Vegetation and MERIS vegetation indices using *in situ* measurements in a semi-arid environment," *IEEE Trans. Geosci. Remote Sens.*, vol. 44, no. 7, pp. 1774–1786, Jul. 2006.

[56] J. Roujean, M. Leroy, A. Podaire, and P. Deschamps, "Evidence of surface reflectance bidirectional effects from a NOAA/AVHRR multi-temporal data set," *Int. J. Remote Sens.*, vol. 13, no. 4, pp. 685–698, 1992.

[57] G. Rondeaux, "Polarisation de la lumire rflchie par un couvert vgtal," Ph.D. dissertation, Universit de Paris, Paris, France, 1990.

[58] X. Li and A. Strahler, "Geometric-optical bidirectional reflectance modeling of the discrete crown vegetation canopy: Effect of crown shape and mutual shadowing," *IEEE Trans. Geosci. Remote Sens.*, vol. 30, no. 2, pp. 276–292, Mar. 1992.

[59] W. C. Snyder, "Structured surface bidirectional reflectance distribution function reciprocity: Theory and counterexamples," *Appl. Opt.*, vol. 41, no. 21, pp. 4307–4313, 2002.

[60] Y. Shuai, C. Schaaf, A. Strahler, J. Liu, and Z. Jiao, "Quality assessment of BRDF/albedo retrievals in MODIS operational system," *Geophys. Res. Lett.*, vol. 35, no. 5, pp. 1–L05 407, 2008.

[61] A. Lattanzio, Y. Govaerts, and B. Pinty, "Consistency of surface anisotropy characterization with Meteosat observations," *Adv. Space Res.*, vol. 39, no. 1, pp. 131–135, 2007.

[62] Y. M. Govaerts, A. Lattanzio, B. Pinty, and J. Schmetz, "Consistent surface albedo retrieval from two adjacent geostationary satellites," *Geophys. Res. Lett.*, vol. 31, no. 15, p. L15201, Aug. 2004.

Authors' photographs and biographies not available at the time of publication.